THINNING OF A BRITTLE CRUST AND LOW-MAGNITUDE PALAEOEARTHQUAKES ALONG THE EASTERN VOLCANIC FRONT, KAMCHATKA

Zelenin[1], E., Kozhurin[2, 1], A.
[1]*Geological Institute RAS, Moscow, Russia*
[2]*Institute of Volcanology and Seismology FEB RAS, Petropavlovsk-Kamchatsky, Russia*

Eastern Volcanic Front (EVF) is the easternmost active volcanic belt of the Central Kamchatka (Fig. 1). Quaternary calderas are concentrated along the volcanic belt. Clearly visible on satellite imagery, fault scarps tend to line up along the belt as well, heavily deforming ignimbrite plateaus of caldera-forming eruptions and extending into caldera-fill deposits. All the faults group in a narrow but continuous graben not exceeding 10 km in width. The most informative transect of the fault zone can be found at the Shirokoe Plateau composed of pyroclastic deposits of 40 ky BP Uzon eruption (Florensky, 1984, Bindeman et al., 2010). We have exploited aerial imagery of the plateau surface to construct stereoscopic images, a digital elevation model (DEM) and an orthomosaic of 1 m spatial resolution, which is detailed enough to determine fault kinematics and estimate offsets at individual fault scarps. Furthermore, some fault segments formed by single event displacements are visible as well. These provide a comprehensive tool for structural study of active faults, supported by field survey and trenching.

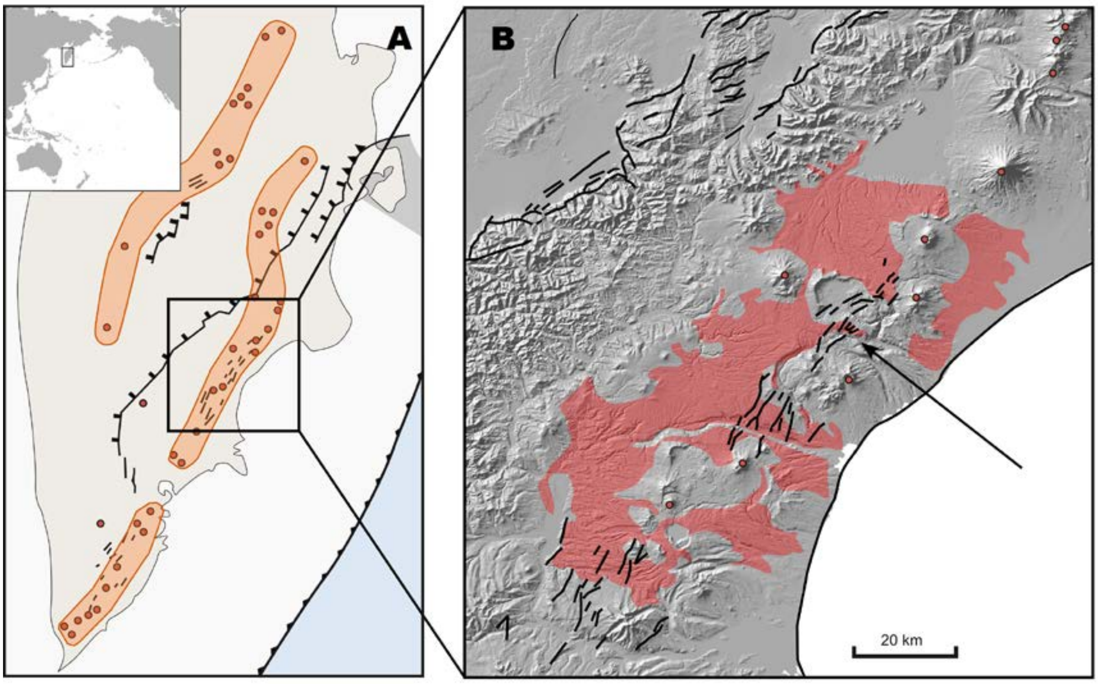

Fig. 1. A, active faults and volcanic belts of Kamchatka. Faults are black lines with hatches for normal faults, triangles for reverse and thrust faults. Orange color marks active volcanic belts and individual volcanoes. B, hillshaded SRTM DEM of the Eastern volcanic front (EVF); transparent red are Pleistocene ignimbrites in the EVF (Bindeman et al., 2010), an arrow on the inset points at the trench site.

We mapped 15 major faults with scarps higher than 1 m and lesser faults, which contribute to the graben as well. To estimate the mean dip angle of faults, we measured fault bends at intersections with landforms on the orthomosaic and DEM. 16 measurements of dip angles yields mean value of 40° ± 8° with normal sense (Kozhurin and Zelenin, 2017). During fieldwork, we excavated and measured one of the fault planes (Fig. 2). Just below the surface, it has reverse sense, but at the trench bottom, it dips 60° towards the downthrown side. Thus, the reverse sense in the upper meter of soil is apparent and may be caused by mass movement down the fault scarp. Antithetic faults and opening fractures in the hanging wall indicate that the fault plane has even shallower dip at depth.

Interpretation of fault segmentation on aerial imagery have some inevitable ambiguity due to scarp degradation after the earthquake. However, none of the fault scarps exceeds 2.5 km in length with mean for major faults comprising 1.7 km. These values are extremely low, and even the worldwide datasets contain few observation of such ruptures (Leonard, 2010, Wells and Coppersmith, 1994). Nonetheless, scaling relations evidence for rupture width comparable to its length, so all the faults deforms less than upper 3 km of the crust. The width of the symmetrical graben is just 4 km, so the easternmost and westernmost faults intersect at a depth of ~ 2.5 km below the surface. There are no sings of the brittle faulting below this level.

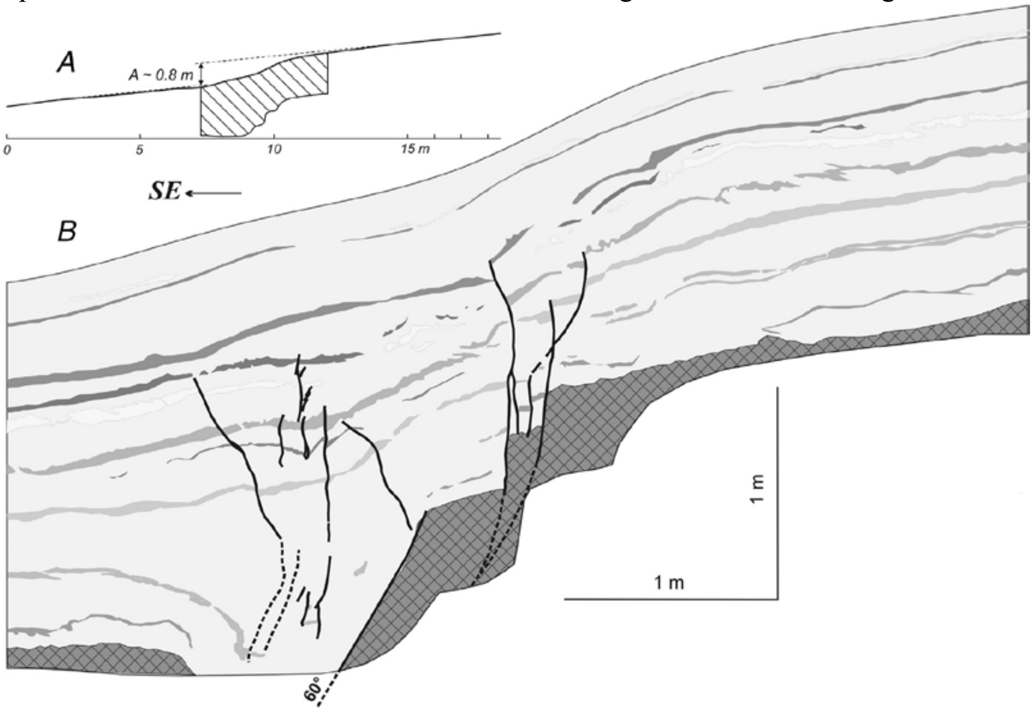

Fig. 2. Faults in the trench wall on the Shirokoye Plateau. A, topographic profile, hatched area is the trench extent. B, log of the southern trench wall. Solid black lines are faults (dashed where uncertain) displacing both Holocene soil-pyroclastic sequence (upper light grey area with tephra layers) and ignimbrite basement (dark grey, cross-hatched). Dip of the main fault plane is indicated.

The thin brittle crust cannot host stronger earthquakes. Scaling relations from (Leonard, 2010), adapted for SI units, link seismic moment M_0 and moment magnitude M_w with rupture length L, rupture area A and mean displacement at a rupture D_{AV}:

$\log(M_0) = 6.10 + 3.0 \log(L)$, $L < 5500$ m, (1)

$M_w = 2/3 \log(M_0) - 6.07$, (2)

$\log(D_{AV}) = 3.39 + 1.33 \log(A)$. (3)

Moment magnitude M_w of such ruptures is 4.4±0.3 (1, 2) and single event displacement is of order 0.1 m (3). We roughly assume earthquake recurrence interval dt to be:

$dt = t_0 D_{AV} / H$, (4)

where t_0 – plateau age, H – fault scarp offset. Thus, the recurrence interval for the highest scarps is of order 300 yrs.

One of the fault planes in the western Shirokoye Plateau was exposed in 2-m deep trench. In the trench wall, the fault deforms soil-pyroclastic sequence with unique tephra layers (Fig. 2), which makes it possible to measure offsets with accuracy of 0.5 cm. Individual accumulated offsets and post-earthquake deposits in the Holocene sequence corresponds to not less than 4 events with displacement 1 to 15 cm. These values agree with the values derived from scaling relations (1-3) and thus strongly supports the thin brittle crust along the volcanic belt.

The same features are typical for the whole fault zone of the EVF: normal faults strike along the axis of volcanic belt and form a n arrow symmetrical graben. However, some external data are needed to corroborate the conclusions due to the absence of detailed structural data for the whole belt. Since none of seismic records provide depth data detailed enough (Kozhurin and Zelenin, 2017), some insights from thermal field could be applied. Both experimental and field data (Handy, 1989) link brittle-ductile transition in the mafic crust to the isotherm of 500°C. The uprising of isotherms is likely to be along the volcanic belt, and the 500°C isotherm may rise to a depth of ca. 5 km, following mantle diapirs (Burov et al., 2003). Thermal section across the EVF compiled by seismic tomography (Gontovaya et al., 2009) supports the isotherm rise well above 20 km.

Considering that extensional faulting is expressed throughout active island arc of Kamchatka, both in the EVF and off it (Fig. 1), we conclude that the whole-regional extension is caused by subduction zone retreat and the described faulting features are induced by superposition of extensional stress field and brittle crust thinning along the Eastern Volcanic Front.

The research was supported by grant 16-05-00090 from the Russian Foundation for Basic Research (RFBR) to Kozhurin.

References

Bindeman I.N., Leonov V.L., Izbekov P.E., Ponomareva V.V., Watts K.E., Shipley N.K., Perepelov A.B., Bazanova L.I., Jicha B.R., Singer B.S., Schmitt A.K., Portnyagin M.V., Chen C.H. Large-volume silicic volcanism in Kamchatka: Ar–Ar and U–Pb ages, isotopic, and geochemical characteristics of major pre-Holocene caldera-forming eruptions // Journal of Volcanology and Geothermal Research, 2010. Vol. 189. № 1. Pp. 57–80.

Burov E., Jaupart C., Guillou-Frottier L. Ascent and emplacement of buoyant magma bodies in brittle-ductile upper crust // Journal of Geophysical Research: Solid Earth, 2003. Vol. 108. № B4. Pp. 1-20.

Florensky, I.V., 1984. On the age of Uzon and Krashenninnikov calderas // Vulkanologiya i Seismologiya. № 1, Pp. 102–106 (in Russian).

Gontovaya L.I., Gordienko V.V., Gordienko L.Ya. A Density Model of the tectonosphere in the transition zone of ocean type, the Kamchatka region // Geology and Mineral resources of the World Ocean, 2009. № 4. Pp. 16-26.

Handy M.R. Deformation regimes and the rheological evolution of fault zones in the lithosphere: the effects of pressure, temperature, grainsize and time // Tectonophysics, 1989. Vol. 163. № 1-2. Pp. 119-152.

Kozhurin A.I., Zelenin E.A. An extending island arc: the case of Kamchatka // Tectonophysics, 2017. Vol. 706-707. Pp. 91-102.

Leonard M. Earthquake fault scaling: Self-consistent relating of rupture length, width, average displacement, and moment release // Bulletin of the Seismological Society of America, 2010. Vol. 100. № 5A. Pp. 1971-1988.

Wells D. L., Coppersmith K. J. New empirical relationships among magnitude, rupture length, rupture width, rupture area, and surface displacement // Bulletin of the seismological Society of America, 1994. Vol. 84.№ 4. Pp. 974-1002.